© 2015. Published by The Company of Biologists Ltd | Journal of Cell Science (2015) 128, 1217–1229 doi:10.1242/jcs.165746

RESEARCH ARTICLE

Decatransin, a new natural product inhibiting protein translocation at the Sec61/SecYEG translocon

Tina Junne[1], Joanne Wong[2], Christian Studer[2], Thomas Aust[2], Benedikt W. Bauer[3,4], Martin Beibel[2], Bhupinder Bhullar[2], Robert Bruccoleri[5], Jürg Eichenberger[2], David Estoppey[2], Nicole Hartmann[2], Britta Knapp[2], Philipp Krastel[2], Nicolas Melin[2], Edward J. Oakeley[2], Lukas Oberer[2], Ralph Riedl[2], Guglielmo Roma[2], Sven Schuierer[2], Frank Petersen[2], John A. Tallarico[6], Tom A. Rapoport[3,4], Martin Spiess[1,*] and Dominic Hoepfner[1,2,*]

ABSTRACT

A new cyclic decadepsipeptide was isolated from *Chaetosphaeria tulasneorum* with potent bioactivity on mammalian and yeast cells. Chemogenomic profiling in *S. cerevisiae* indicated that the Sec61 translocon complex, the machinery for protein translocation and membrane insertion at the endoplasmic reticulum, is the target. The profiles were similar to those of cyclic heptadepsipeptides of a distinct chemotype (including HUN-7293 and cotransin) that had previously been shown to inhibit cotranslational translocation at the mammalian Sec61 translocon. Unbiased, genome-wide mutagenesis followed by full-genome sequencing in both fungal and mammalian cells identified dominant mutations in Sec61p (yeast) or Sec61α1 (mammals) that conferred resistance. Most, but not all, of these mutations affected inhibition by both chemotypes, despite an absence of structural similarity. Biochemical analysis confirmed inhibition of protein translocation into the endoplasmic reticulum of both co- and post-translationally translocated substrates by both chemotypes, demonstrating a mechanism independent of a translating ribosome. Most interestingly, both chemotypes were found to also inhibit SecYEG, the bacterial Sec61 translocon homolog. We suggest 'decatransin' as the name for this new decadepsipeptide translocation inhibitor.

KEY WORDS: SEC61, Endoplasmic reticulum, Translocation inhibition, Haploinsufficiency profiling, Target identification, Cotransin

INTRODUCTION

Most secretory and membrane proteins are translocated across or inserted into the plasma membrane of bacteria or the endoplasmic reticulum of eukaryotes by the conserved SecY/Sec61 translocon complex (Park and Rapoport, 2012; Shao and Hegde, 2011). The core translocon consists of SecY or Sec61α (Sec61p in yeast) in bacteria and eukaryotes, respectively, forming a protein-conducting channel with its ten transmembrane domains (TM1–TM10), and of two peripherally attached single- to triple-spanning subunits SecG or Sec61β (Sbh1p), and SecE or Sec61γ (Sss1p). In its idle state, the potential pore is closed by a central constriction ring of six predominantly hydrophobic residues and a lumenal plug helix that blocks the periplasmic or luminal cavity. Substrate proteins are targeted either co- or post-translationally to the SecYEG/Sec61 complex. In the former case, a hydrophobic signal sequence is recognized by signal recognition particle (SRP) to bring the nascent-chain–ribosome complex to the SRP receptor in the appropriate membrane allowing the ribosome to bind to cytoplasmic loops of SecY/Sec61α. Alternatively, substrates are synthesized into the cytosol and reach the translocon post-translationally, which, in eukaryotes involves the Sec62–Sec63–Sec66–Sec72 complex. Somehow the signal sequence engages with the translocon and intercalates as a helix in between TM2 and TM7 of SecY/Sec61α, which form a lateral gate into the lipid bilayer (Gogala et al., 2014; Park et al., 2014; Voorhees et al., 2014) In the process, the hydrophilic sequence is inserted into the pore, pushing away the plug and the constriction residues that act as a gasket around the polypeptide (Park and Rapoport, 2011). It is not clear how signal peptides with diverse primary sequences that only share a general hydrophobic character initiate translocation.

Chemical inhibitors have frequently been useful tools to elucidate the molecular mechanisms of complex processes. A general translocation inhibitor is eeyarestatin, a chemical most likely binding to the translocon and preventing the transfer of the nascent-chain–ribosome complex from the SRP–SRP receptor targeting complex to the translocon in mammalian cells (Cross et al., 2009). Apratoxin A, a cyanobacterial metabolite, has been shown to inhibit cotranslational translocation *in vitro* (Liu et al., 2009), but the blocked step is unknown. Furthermore a group of closely related cyclic heptadepsipeptide inhibitors including HUN-7293, CAM741 (Besemer et al., 2005) and a simplified version thereof called cotransin (Garrison et al., 2005) have been found to inhibit cotranslational translocation of VCAM1 and other specific substrates (Maifeld et al., 2011; Westendorf et al., 2011). Photoaffinity labeling has identified Sec61α as the target (MacKinnon et al., 2007), which was confirmed by isolation of resistance mutations in *SEC61A1* (MacKinnon et al., 2014). Using *in vitro* translation–translocation assays, it has been shown that SRP-dependent targeting and binding of the ribosome, and interaction of the signal with the translocon in the cytosolic vestibule, are unaffected by these cyclic heptadepsipeptide inhibitors, but signal insertion is blocked (Besemer et al., 2005; Garrison et al., 2005; MacKinnon et al., 2014). The origin of signal specificity of inhibition is not clear (Harant et al., 2006).

[1]Biozentrum, University of Basel, Klingelbergstrasse 50/70, 4056 Basel, Switzerland. [2]Novartis Institutes for BioMedical Research, Novartis Campus, 4056 Basel, Switzerland. [3]Howard Hughes Medical Institute, Harvard Medical School, 240 Longwood Avenue, Boston, MA 02115, USA. [4]Department of Cell Biology, Harvard Medical School, 240 Longwood Avenue, Boston, MA 02115, USA. [5]Congenomics, LLC, 60 Gates Farm Road, Glastonbury, CT 06033, USA. [6]Novartis Institutes for BioMedical Research, 250 Massachusetts Avenue, Cambridge, MA 02139, USA.

*Authors for correspondence (martin.spiess@unibas.ch; dominic.hoepfner@novartis.com)

Received 6 November 2014; Accepted 15 January 2015

Journal of Cell Science (2015) 128, 1217–1229 doi:10.1242/jcs.165746

In this study we identified a new bioactive cyclodepsipeptide that inhibits cell growth. To identify its target, we used yeast chemogenomic profiling and unbiased genome-wide mutagenesis, followed by selection and sequencing of resistant clones in yeast and mammalian cells. All assays identified the endoplasmic reticulum (ER) translocon component Sec61 as the conserved target in eukaryotic cells. Biochemical characterization of the inhibition mechanism in both yeast and mammalian cells indicated that the compound blocks all translocation through the Sec61 channel. We thus suggest 'decatransin' as the name for this new decadepsipeptide translocation inhibitor.

RESULTS

Isolation of a new decadepsipeptide from *Chaetosphaeria tulasneorum* with potent biological activity

Screening new compounds of natural origin for growth inhibition of HCT116 human carcinoma cells identified compounds of the saprophyte fungus *Chaetosphaeria tulasneorum* with potent activity. Scaled up cultivation, isolation, purification and structure elucidation (see Materials and Methods as well as supplementary materials) led to the discovery of a cyclic decadepsipeptide (Compound 1, Fig. 1A).

The presence of the non-proteinogenic amino acids pipecolic acid and homoleucine at positions 2, 6 and 9, and 3, 4 and 7, respectively, indicated that the compound had been synthesized by a non-ribosomal peptide synthetase (NRPS). NRPSs are large multienzymes with a modular organization of catalytic domains, namely the adenylation (A), peptidyl carrier protein (PCP) and condensation (C) domains, responsible for the activation of, transfer of amino acids as thioesters and peptide bond formation, respectively. Using a software to predict microbial natural product pathways (Bachmann and Ravel, 2009), multiple NPRSs were identified in the genome of *Chaetosphaeria tulasneorum*. The NRPS responsible for the biosynthesis of the compound was expected to contain ten modules and four N-methyltransferases. Of the predicted NRPSs, three contained ten modules. The pattern of eight-residue signature sequences that define A-domain selectivity (Stachelhaus et al., 1999) uniquely identified a single NRPS with DPFMYLGI in the A domains at positions 2, 6 and 9, and DAWTYGVA at positions 3, 4 and 7, corresponding to the positions of pipecolic acids and homoleucines, respectively (Fig. 1A,B). In addition, N-methyltransferases were present at positions 4, 5, 7 and 10, consistent with the observed N-methylation patterns. Finally, the synthetase had a terminal condensation domain (C_T) catalyzing the cyclization of NRPS products in fungi (Gao et al., 2012). The presence of a 2-hydroxy-acid dehydrogenase gene in the neighborhood of the NRPS (Fig. 1C) supported incorporation of a 2-hydroxy-amino acid at position 1, and thus peptide closure through an intermolecular ester bond, which is the hallmark of the depsipeptide family. Genes encoding L-pipecolate oxidase and 2-isopropylmalate synthase were also found close to this megasynthetase gene (Fig. 1C; supplementary material Table S1). These genes are likely involved in pipecolic acid and homoleucine biosynthesis, respectively (Field et al., 2004; He, 2006). In summary, sequence analysis identified the NRPS and accessory genes involved in the synthesis of the decadepsipeptide.

Yeast chemogenomic profiling identifies the Sec61 translocon complex as the site of action

Although the compound showed potent growth inhibition of mammalian cell lines, such as HCT116 human colon carcinoma cells and COS-1 monkey kidney cells at IC_{50} 30–140 nM, it also inhibited growth of the yeast *S. cerevisiae* at IC_{50} ~2 µM (Fig. 1A), thus enabling us to apply chemogenomic profiling to identify target proteins or pathways (Giaever et al., 1999). Haploinsufficiency profiling (HIP) and homozygous profiling (HOP) are based on *S. cerevisiae* heterozygous and homozygous deletion collections (Hoon et al., 2008). HIP indicates proteins or pathways directly affected by the compound, whereas HOP reveals synthetic effects and identifies compensating factors or pathways. The results are visualized by plotting the relative growth reduction of individual strains by the compound (sensitivity) versus a measure of significance (*z*-score, see Materials and Methods). The cyclic decadepsipeptide produced profiles that revealed haploinsufficiency for all components of the Sec61–Sec63 core complex (Fig. 2A, HIP), as well as synthetic growth defects after homozygous deletion of the three non-essential genes *SBH1*, *SEC66* and *SEC72* of the Sec61–Sec63 complex (Fig. 2A, HOP). This strongly indicated that the Sec61–Sec63 translocon is the target of the inhibitor. Dose–response growth experiments using individual strains with compound 1 fully validated the HIP result (supplementary material Fig. S1B). The only other hypersensitive HIP strain of the original library, CWC21 (involved in RNA splicing), was found to contain a heterozygous frame-shift mutation in the *SEC63* gene responsible for the phenotype (supplementary material Fig. S2).

Comparing the decadepsipeptide profile to archived datasets identified a striking similarity with the HIP and HOP profile of a cyclic heptadepsipeptide, denoted compound 2 (Fig. 2B,C). Structural similarity searches with compound 1 did not reveal any similarity to compound 2 [Tanimoto coefficient <0.25 for the entire molecule, and 0.26 when only comparing the scaffolds (Bender and Glen, 2004)] or any other relevant hits, indicating that they constitute distinct chemotypes. However, the structure of compound 2 is almost identical to HUN-7293 and its derivatives, the cotransins, which have been previously characterized as mammalian translocon inhibitors (Besemer et al., 2005; Garrison et al., 2005) (Fig. 2B). With an IC_{30} of 200 µM, HUN-7293 was less effective on wild-type yeast than compound 2 and the decadepsipeptide by a factor of 30 and 100, respectively, but produced very similar HIP and HOP profiles at this higher concentration (Fig. 2D). Pairwise comparison of HIP *z*-scores (Fig. 2F) confirmed conserved hits and thus the conserved mechanism of action of the new decadepsipeptide and the heptadepsipeptide and cotransin chemotype. It is interesting to note that prominent hits in the HOP profiles of the decadepsipeptides were strains where *IPT1* (inositolphosphotransferase) or *SUR1* (mannosylinositol phosphorylceramide synthase) have been deleted, suggesting a new genetic link between the Sec61–Sec63 translocon and lipid metabolism.

Genome-wide mutagenesis in yeast identifies mutations in Sec61 that confer resistance

To identify the direct target of the inhibitors using an orthogonal approach, we performed unbiased, genome-wide chemical mutagenesis and selection for resistance to the inhibitors in parallel for *S. cerevisiae* and for mammalian HCT116 cells. In drug-efflux-compromised yeast, we obtained 45 colonies resistant to 30 µM compound 1. These resistant cells were mated with wild-type cells, and the heterozygous clones maintained the resistance, indicating that the underlying mutations were dominant. Direct Sanger sequencing of the *SEC61*, *SEC62* and *SEC63* gene loci revealed 13 different single-amino acid mutations exclusively in *SEC61* (Fig. 3A, top; Table 1). The

Journal of Cell Science (2015) 128, 1217–1229 doi:10.1242/jcs.165746

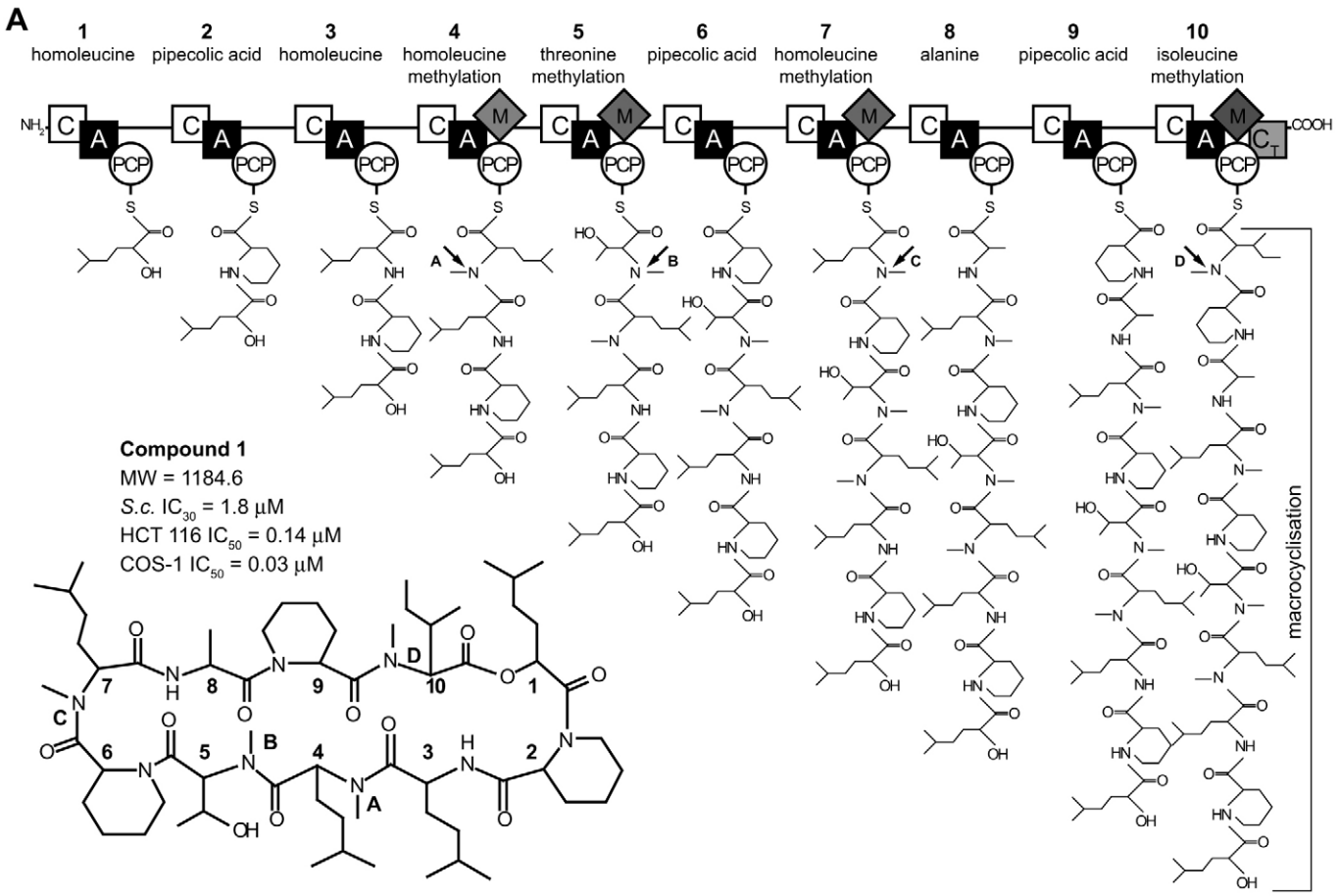

B

position	proposed aa	A-domain signature	C-domain coordinates	A-domain coordinates	PCP coordinates	additional domain coordinates
	homoleucine-derived					
1	2-hydroxy carboxylic acid	GAVVVGVS	54-303	629-830	1048-1092	
2	pipecolic acid	DPFMYLGI	1104-1542	1715-1918	2117-2180	
3	homoleucine	DAWTYGVA	2202-2630	2805-3014	3204-3267	
4	homoleucine	DAWTYGVA	3289-3717	3890-4099	4700-4763	M: 4199-4631
5	threonine	DAWLLSST	4787-5213	5388-5597	6195-6258	M: 5695-6126
6	pipecolic acid	DPFMYLGI	6280-6708	6881-7084	7282-7345	
7	homoleucine	DAWTYGVA	7367-7795	7968-8177	8772-8835	M: 8271-8703
8	alanine	DVWTLAAI	8857-9285	9458-9667	9857-9920	
9	pipecolic acid	DPFMYLGI	9942-10370	10543-10746	10944-11007	
10	isoleucine	DAWFFGVT	11029-11457	11630-11839	12343-12497	M: 11933-12365 C_T: 12549-12827

Fig. 1. Structure and biosynthesis of a novel bioactive decadepsipeptide. (A) Structure, molecular mass and growth inhibition potency of compound 1, a new decadepsipeptide produced by *Chaetosphaeria tulasneorum*. Dose–response curves for HCT116 and yeast cells are shown in Fig. 4B and supplementary material Fig. S1. In addition, the domain organization and proposed assembly line of the matching NPRS is shown. A, adenylation; C, condensation; C_T, terminal condensation; PCP, peptidyl carrier protein; M, methylation. Backbone methylations are labelled A–D in the structures. The peptide intermediates are attached as thioesters to the PCP domains. (B) Modules and specificity signatures of the A-domain binding pockets in the matching NPRS. (C) Genomic context of the NRPS for the decadepsipeptide (Orf3): Orf2, pipecolate oxidase; Orf4, 2-hydroxyacid dehydrogenase; Orf5, 2-isopropylmalate synthase; Orf1 and Orf6, other NRPSs. DNA and protein sequences are provided in supplementary material Table S1.

mutant alleles were introduced into drug-efflux-compromised wild-type cells, replacing the wild-type copy of *SEC61*. The resulting cells were all viable and retained resistance equivalent to the original resistant colonies, demonstrating that the *SEC61* gene encoded the critical target of compound 1. Several mutations increased the IC_{50} value by more than 100-fold,

Journal of Cell Science (2015) 128, 1217–1229 doi:10.1242/jcs.165746

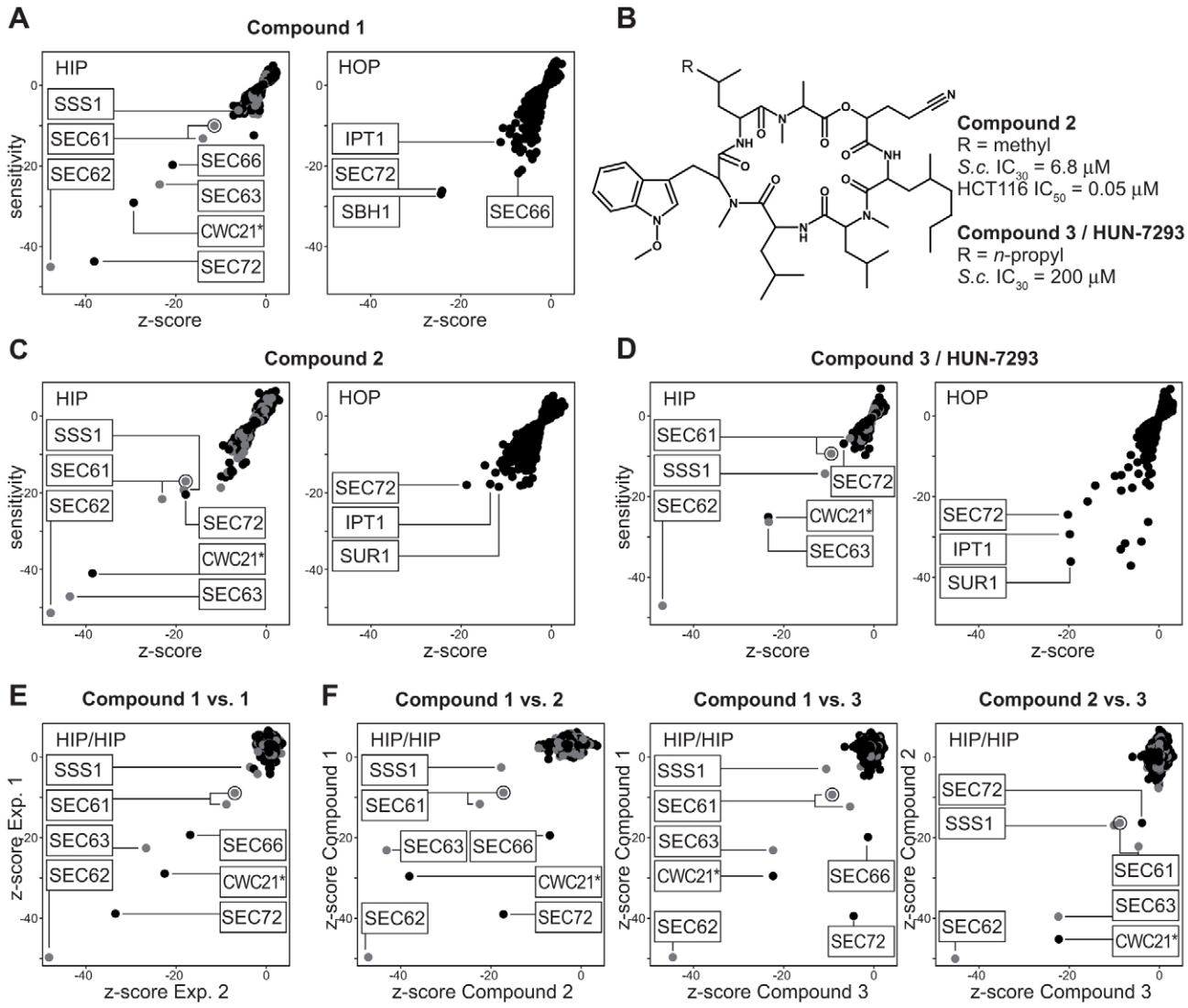

Fig. 2. HIP and HOP suggest that the compounds inhibit the Sec61–Sec63 translocon. (A) HIP HOP profile of the decadepsipeptide compound 1, plotting sensitivity versus *z*-score. Gray and black dots represent strains with deletions in essential and non-essential genes, respectively. HIP and HOP strains related to Sec61–Sec63 translocon function are prevalent. The dubious ORF YLR379w is labeled with a circle and grouped with the SEC61 HIP strain because it substantially overlaps with the *SEC61* gene and its deletion affects both ORFs. The CWC21 strain is marked with an asterisk because follow-up analysis revealed that hypersensitivity of this strain is not due to the heterozygous *CWC21* deletion but to a *SEC63* background mutation (supplementary material Fig. S2). (B) Structure and activity of a new heptadepsipeptide compound 2 and of the closely related known translocation inhibitor compound 3 (HUN-7293). (C,D) HIP and HOP profiles of the two heptadepsipeptides as described for A. (E) Reproducibility of HIP profiling is demonstrated by *z*-score alignment of two independent experiments with compound 1. (F) Comparison of the activities of compounds 1–3 by pair-wise HIP *z*-score alignment.

whereas others only caused moderate increases in the inhibitory concentration (Table 1; Fig. 3B). Given that the Sec61 translocon had also been shown to be the target of the heptadepsipeptide chemotype (compound 2, compound 3; HUN-7293 and cotransin), we tested for cross-resistance to compound 2. Except for mutations G97D, A186T and G430D, which were completely sensitive to compound 2, the mutants were cross-resistant to compound 2 (Table 1; Fig. 3C). This indicates similar, yet distinct, modes of action of the deca- and hepta-depsipeptide inhibitors on Sec61. In addition, we also tested our existing library of Sec61p mutants that had been isolated in the context of membrane protein topogenesis (Junne et al., 2007) with respect to sensitivity to compounds 1 and 2 (supplementary material Fig. S3). Mutation of the six residues of the constriction ring, partial and full deletion of the plug domain, and deletion of TM2 also resulted in strong resistance to both inhibitors.

Genome-wide mutagenesis in mammalian cells supports target conservation

We also performed genome-wide mutagenesis of human HCT116 cells using ethyl methanesulfonate (EMS) and N-ethyl-N-nitrosourea (ENU). Owing to limited availability of the new decadepsipeptide, mutagenized cells were cultured in the presence of 1 µM compound 2. After 2 weeks, 12 strongly growing colonies were picked for further characterization. The majority of the clones showed more than 20-fold increased IC_{50} for compound 2 (Fig. 4A). With the exception of one single clone, they also were cross-resistant to compound 1, however,

Journal of Cell Science (2015) 128, 1217–1229 doi:10.1242/jcs.165746

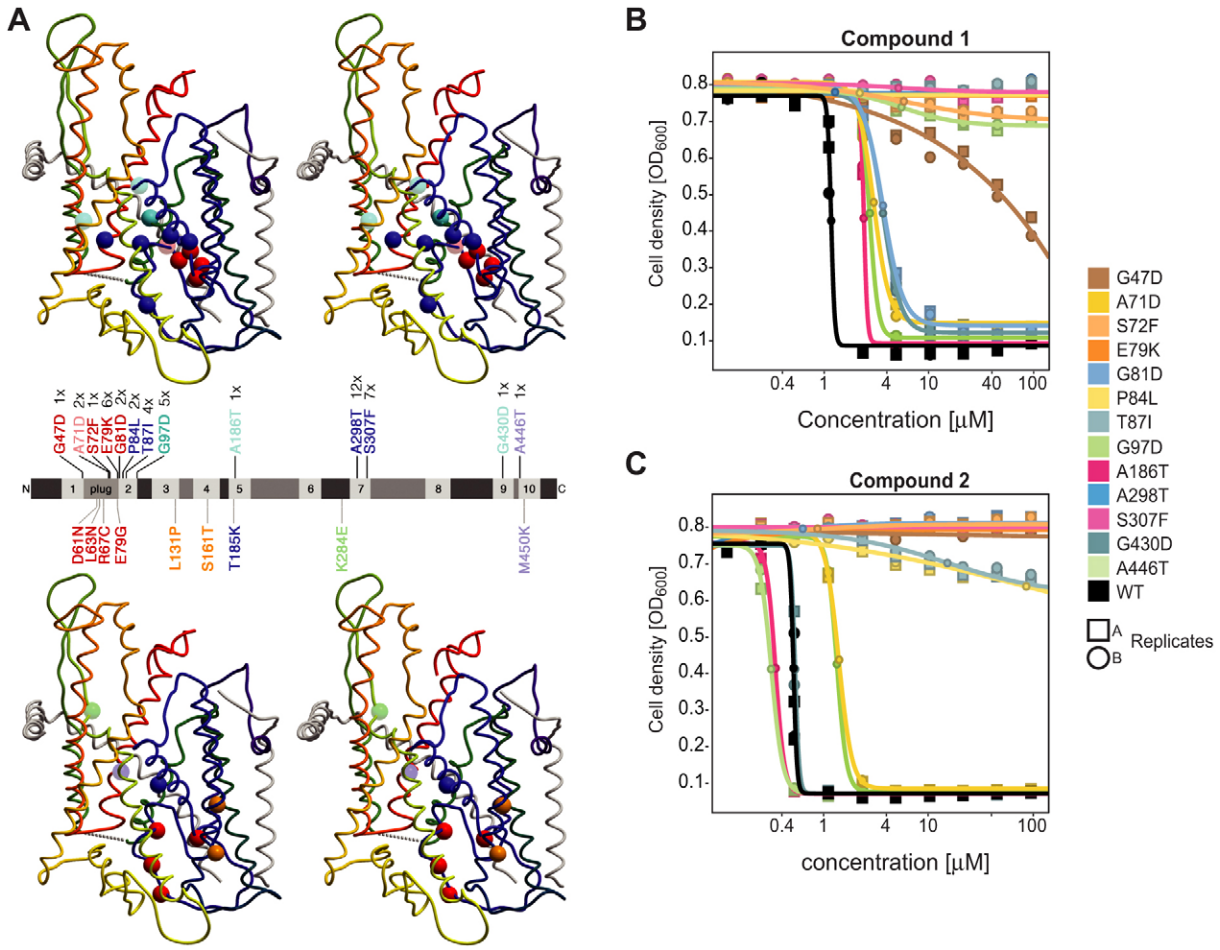

Fig. 3. Selection of yeast mutants resistant to the inhibitors. (A) Thirteen different single amino acid mutations were identified in *SEC61* of chemically mutagenized drug-efflux-compromised yeast cells selected for resistance to 30 μM compound 1 on plates. Their positions are indicated in the model of the yeast Sec61 complex (Junne et al., 2006) shown in stereo in the top panel. Below, previously studied Sec61p single point mutants that were found to be resistant (see Table 2) are similarly presented. In the middle, the Sec61p sequence is schematically shown as a bar with numbered transmembrane domains. The newly selected and the old resistance mutations are indicated above (with their frequency of occurrence) and below, respectively. Mutations resistant to both compounds 1 and 2 are shown in red if they have a *prl* phenotype, and in blue if not. Mutations resistant only to compound 1 (not *prl*) are shown in cyan, those resistant only to compound 2 in green (not *prl*) or orange (*prl*). The weak mutants are indicated by lighter shades. (B,C) Dose–response curves of wild-type yeast strains in liquid cultures expressing the indicated Sec61p point mutants for compound 1 and compound 2, respectively. Moderate to high resistance to compound 1 (against which they were originally selected) was validated for all mutations. They were also resistant to compound 2, with the notable exception of G97D, A186T and G430D. Resulting IC_{50} and r^2 values are listed in Table 1. Boxes and circles indicate independent replicate experiments. Dose–response curves for resistant mutants shown in the lower part of A are presented in supplementary material Fig. S3.

most of them only had a 2–3-fold increased IC_{50} values (Fig. 4B). Resistance was specific because no change was observed in sensitivity to the control compound taxol (Fig. 4C).

To identify the resistance-conferring mutations, the genomic DNA was isolated from ten resistant clones and two sensitive parental samples, and used to prepare exon-enriched libraries for Illumina sequencing. The resulting reads were aligned to the human genome, and variants [single nucleotide polymorphisms (SNPs) and insertions/deletions (indels)] were called for each of the samples and then filtered according to several quality metrics (e.g. sequencing depth). Variants in the parental sample were excluded. For further analysis, we considered only missense and nonsense mutations in coding regions. We further excluded missense SNPs that were not predicted to be deleterious to protein function (see Materials and Methods). Finally, we included only mutations in genes that were expressed according to RNAseq analysis of the parental samples. Applying these three filters, the gene with the highest number of mutations was *SEC61A1*, which encodes Sec61α1, the human ortholog of yeast Sec61, with mutations in eight out of the ten clones (Fig. 4D). Based on the SNP patterns, the ten clones originated from eight independent progenitors. The two M65R and two D60E clones showed highly similar SNP patterns, whereas the patterns of the two S71F clones indicated independent events (Table 3). We further sequenced the *SEC61A1* cDNA of six additional resistant HCT116 clones obtained by N-ethyl-N-nitrosourea (ENU) mutagenesis, all six of which also harbored mutations (Table 3). The mutated residues D60, R66 and S71 of human Sec61α1 correspond to D61, R67 and S72 in yeast Sec61p, which also produced resistance when mutated (Fig. 3). Thus the identical mutations S71F in Sec61α1 and S72F in Sec61p have even been identified independently in different species, although yielding different levels of resistance. In summary, selection for resistant clones identifies the Sec61 translocon as the conserved target of deca- and hepta-depsipeptide inhibitors in both yeast and mammalian cells.

Journal of Cell Science (2015) 128, 1217–1229 doi:10.1242/jcs.165746

Table 1. Inhibitor sensitivity of yeast Sec61p mutants selected by their resistance to compound 1

Sec61 mutation	Color code[a]	*prl*	CPY translation defect	Compound 1				Compound 2			
				IC_{50}[b] (μM)	r^{2c}	IC_{50} ratio to control	Phenotype	IC_{50}[b] (μM)	r^{2c}	IC_{50} ratio to control	Phenotype
Wild-type	–	–	–	1.2	0.985	1	S	0.5	0.980	1	S
G47D	Red	+	–	100	0.977	83	R	>200	–	>100	R
A71D	Red	+	–	3	0.996	2.5	(R)	1.4	0.999	2.8	(R)
S72F	Red	+	–	>200	–	>100	R	>200	–	>100	R
E79K	Red	+	–	>200	–	>100	R	>200	–	>100	R
G81D	Red	+	–	3.6	0.997	3	(R)	>200	–	>100	R
P84L	Blue	–	–	>200	–	>100	R	>200	–	>100	R
T87I	Blue	–	–	>200	–	>100	R	>200	–	>100	R
G97D	Cyan	–	–	>200	–	>100	R	0.3	0.997	0.6	S
A186T	Cyan	–	–	2.4	0.993	2	(R)	0.3	0.998	0.6	S
A298T	Blue	–	–	>200	–	>100	R	>200	–	>100	R
S307F	Blue	–	–	>200	–	>100	R	>200	–	>100	R
G430D	Cyan	–	–	3.7	0.996	3.1	(R)	0.5	0.986	1	S
A446T	Blue	–	–	2.7	0.995	2.3	(R)	1.3	0.999	2.6	(R)

The Sec61p mutants isolated as resistant to compound 1 were tested for the *prl* phenotype and CPY translocation defects as in Junne et al. (Junne et al., 2007). S, sensitive; R, resistant (IC_{50} at least 50-fold higher than wild-type); (R), moderately resistant (IC_{50} at least two-fold higher than wild-type). [a]The color code of mutations conferring resistance to at least one compound corresponds to that used in Fig. 3A, lower panel; [b]corresponding IC_{50} curves are shown in supplementary material Fig. S3; [c]r^2 values are shown where a sigmoidal curve could be fitted.

The compounds inhibit both co- and post-translational protein translocation into the ER

To test translocon function directly in the presence or absence of these compounds, yeast cells were metabolically labeled with [^{35}S]methionine for 5 min, and translocation of dipeptidylaminopeptidase B (DPAPB) and carboxypeptidase Y (CPY) into the ER was assessed based on the glycosylation and processing pattern after immunoprecipitation and SDS-PAGE. DPAPB and CPY are established co- and post-translationally translocated substrates, respectively. Both the decadepsipeptide compound 1 and the heptadepsipeptide compound 2 effectively inhibited co- and post-translational translocation as is apparent in a reduction of the glycosylated and an increase of the unglycosylated forms (Fig. 5A). Inhibition of post-translational translocation demonstrates that the mechanism of action is independent of SRP and SRP receptors and thus of protein targeting to the translocon, as has already been concluded for the cotransins from *in vitro* translation–translocation experiments (Garrison et al., 2005), and is independent of the presence of a translating ribosome.

Inhibition was dependent on the concentration (Fig. 5B) as well as on pre-incubation time (Fig. 5C,D): compound 2 required ~30 min to reach maximal levels, and compound 1 even longer. This time dependence most likely reflects the penetration kinetics of the compounds (the time required to cross the cell wall and plasma membrane). In general, CPY translocation appeared to be more sensitive to inhibition than that of DPAPB.

Both types of inhibitors also acted on non-natural, generic signal sequences made of 13 or 16 consecutive leucine residues (Fig. 5E). This underlines the independence of the action mechanism of these inhibitors from the specific signal sequence in yeast. In agreement with the target conservation in mammalian cells, both compounds similarly inhibited translocation in mammalian COS-1 cells, as shown in Fig. 5F for the asialoglycoprotein receptor H1, a type II membrane protein, and derivatives with generic signal-anchors made of Leu_{13} or Leu_{25} segments.

Cross-species activity allows detection of a putative, conserved binding site

The conserved action of both chemotypes on the fungal and human Sec61p homologs and conserved mutations that confer resistance across species raised the question as to whether bacterial translocons also can be targeted by compounds 1 and 2. We performed *in vitro* translocation experiments on purified *E. coli* translocons reconstituted into lipid membranes as described previously (Bauer et al., 2014). Both compounds inhibited translocation of a pro-OmpA model substrate in a dose-dependent fashion (Fig. 5G) with estimated IC_{50} of 10 μM for compound 1 and 90 μM for compound 2. Interestingly, deletion of the SecY plug domain conferred resistance to both chemotypes as shown by a considerable shift of the curves.

Most *prl* mutations confer resistance to Sec61 inhibitors

The identified resistance-conferring mutations are conspicuously concentrated in or close to the plug domain (Fig. 3A; Fig. 4D, and see MacKinnon et al., 2014). Plug mutations have previously been found to cause a *prl* phenotype, i.e. the suppression of signal sequence mutations (Emr et al., 1981). *prl* mutations specifically destabilize the closed state of the translocon, and thereby facilitate pore opening, reducing the stringency for signal acceptance by the translocon. We tested the new resistant Sec61p mutants for a *prl* phenotype. Five of the 13 newly isolated resistant mutants indeed suppressed the translocation defect of CPYΔ3 in which the hydrophobic core of the signal peptide was truncated by three residues (Fig. 5H). All of them carry mutations involving the plug, four in the plug domain itself and one (G47D) in TM1 pointing towards it. From our older collection (Table 2), all *prl* mutants except one (I86T) were significantly resistant to at least one of the inhibitors. The correlation between the *prl* phenotype and resistance suggests that the inhibitors bind to the closed state of the wild-type translocon. In *prl* mutants this state is destabilized, resulting in reduced binding affinity for the compounds.

Journal of Cell Science (2015) 128, 1217–1229 doi:10.1242/jcs.165746

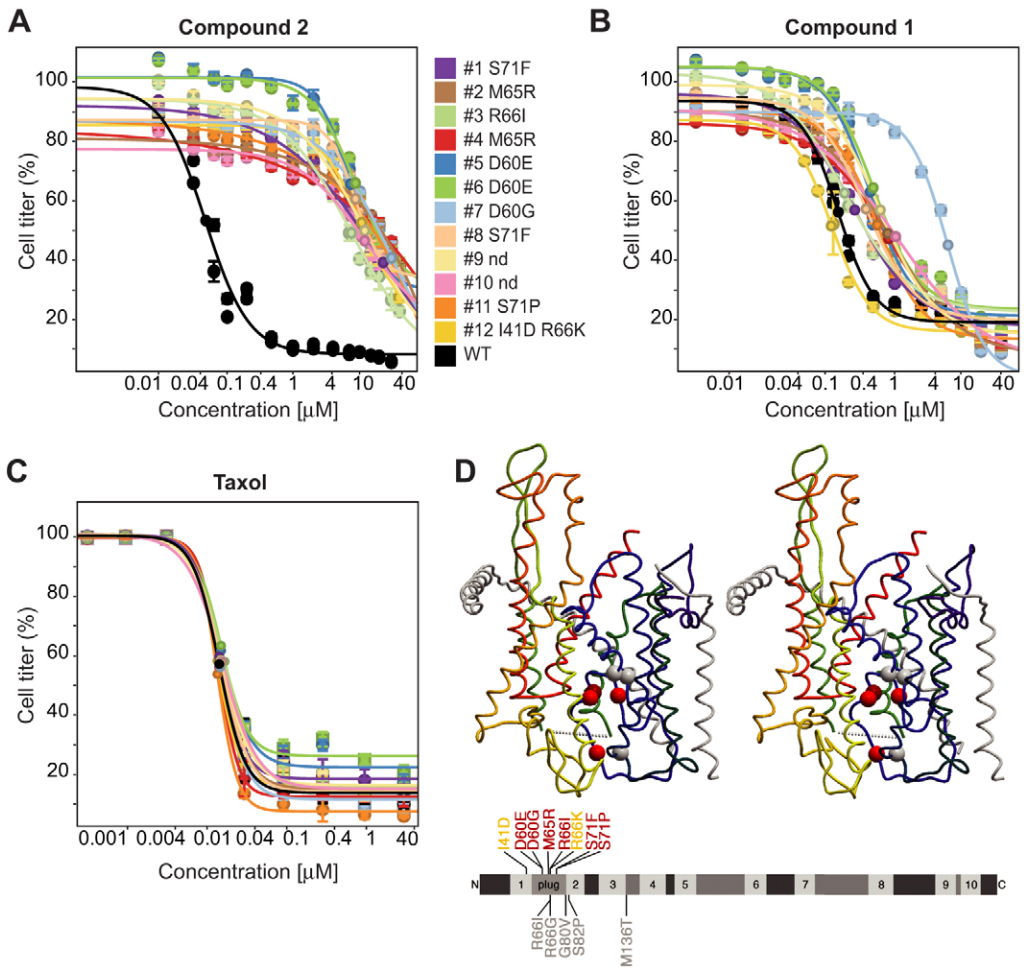

Fig. 4. Selection of resistant mutants in human cells. HCT116 cells were mutagenized and selected for resistance to compound 2. Dose–response validation of 12 resistant clones with identified *SEC61A1* mutations against compounds 2 (A) and 1 (B), and against taxol (C). The mean±s.d. of triplicate determinations are shown. The mutations selected here for resistance to compound 2 and of the recently identified mutations by MacKinnon et al. (MacKinnon et al., 2014) conferring resistance to cotransin CT08 [Maifeld et al., 2011; a compound closely related to compound 3 (HUN-7293)] are shown in the stereo model of the human Sec61 complex in in red and gray, respectively. Below, Sec61α1 is shown as a bar with its transmembrane domains numbered. Red, the single mutations; yellow, the double mutation; gray, the mutations shown by MacKinnon et al. (MacKinnon et al., 2014).

DISCUSSION

Here, we present an integrated study of a new bioactive decadepsipeptide from its isolation and the identification of the responsible megasynthetase of the producer organism by genome-sequencing and *in silico* analysis to the determination of the conserved target in yeast and mammalian cells, as well as in bacteria, using genomic assays and biochemical analysis of the inhibited processes. Given that this compound inhibits co- and post-translational translocation across the Sec61/SecYEG translocon, we propose to name it decatransin. The name also alludes to the cotransins, a group of heptadepsipeptide compounds without detectable molecular similarity that have previously been described as mammalian translocon inhibitors.

The activity of decatransin on the yeast *S. cerevisiae* allowed for chemogenomic profiling to rapidly home in on the Sec61 complex as the potential fungal target: our high-resolution HIP and HOP platform (Hoepfner et al., 2014) identified all core subunits of the heptameric translocon complex. Essentially the same profile was obtained for a new yeast active heptadepsipeptide (compound 2) of the cotransin chemotype and for the original inhibitor HUN-7293 (compound 3).

Mutagenesis followed by sequencing of resistant clones confirmed Sec61 as their primary binding protein. Although this approach has a long history in yeast, to our knowledge this is the first study where an unbiased, genome-wide mutagenesis approach, followed by whole-genome-sequencing has identified the drug target in mammalian cells. Although the cotransin target in mammalian cells had already been well documented previously, this analysis was also performed as proof of principle. Wacker et al. (Wacker et al., 2012) have pioneered this approach for two substances with known binding proteins, using spontaneous resistance and total RNA sequencing. However, in that study the approach failed to unambiguously identify the targets. In our case, the analysis yielded Sec61 as the best-scoring candidate. This might be due to our strategy of inducing mutations rather than selecting spontaneously resistant clones. Multiple mutagenesis experiments in fungi and mammalian cells have revealed that there is a bias towards chromosomal aberrations and SNPs in pleiotropic drug-resistance genes if spontaneous mutants are selected and sequenced (Nyfeler et al., 2012; Richie et al., 2013; Sadlish et al., 2013; Shimada et al., 2013). The underlying mechanism might be that amino acid

Journal of Cell Science (2015) 128, 1217–1229 doi:10.1242/jcs.165746

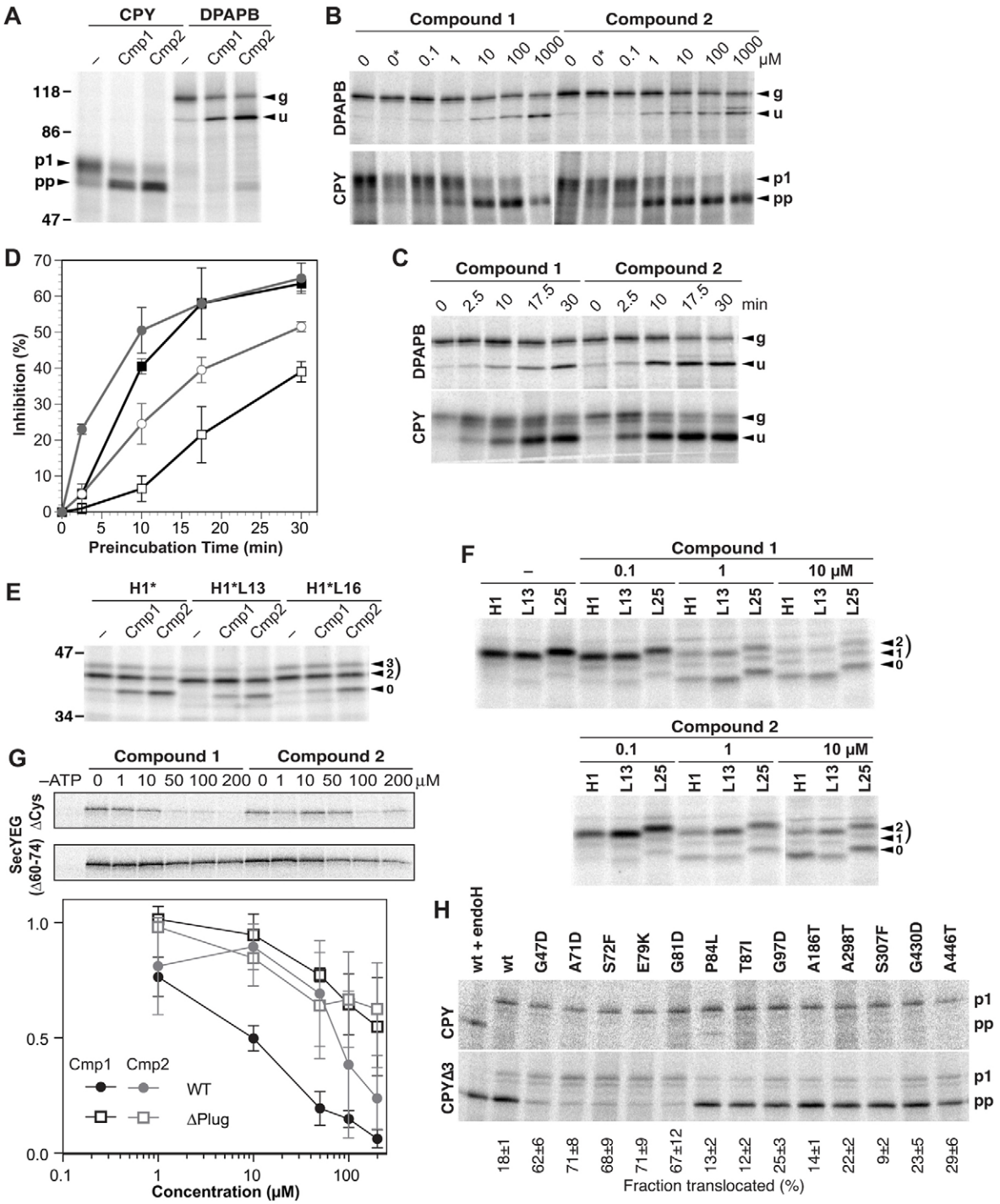

Fig. 5. See next page for legend.

mutations in the essential, primary target can often be deleterious, and these cells are rapidly outcompeted. Thus in the absence of a strong selective pressure there is a bias against spontaneous mutations in these genes, in contrast to drug efflux components or gene copy alterations that have no detrimental phenotype under laboratory conditions.

It has been shown previously that the cotransins allow SRP-dependent targeting and binding of the ribosome–nascent-chain complex to the mammalian translocon (Besemer et al., 2005; Garrison et al., 2005). Our experiments show that decatransin, as well as a member of the cotransin family, are not limited to the inhibition of human or mammalian translocation, but act similarly on fungal and bacterial translocation. Their action is not specific to co-translational (SRP-dependent) translocation, but also inhibits post-translational (SRP-independent) substrates. Thus the presence of a ribosome bound to the translocon complex is not essential.

By extensive *in vitro* crosslinking of arrested nascent chains, MacKinnon et al., (MacKinnon et al., 2014) have recently showed that cotransin prevents the signal sequence from inserting into the

Journal of Cell Science

Journal of Cell Science (2015) 128, 1217–1229 doi:10.1242/jcs.165746

Fig. 5. The compounds inhibit translocation by the yeast, human, and bacterial Sec61/SecYEG translocons. (A) Yeast cells expressing CPY or DPAPB (typical post- and co-translationally translocated substrates, respectively) were preincubated for 30 min with 1% DMSO with or without decadepsipeptide compound 1 (Cmp1) or cotransin heptadepsipeptide compound 2 (Cmp2) to a final concentration of 100 μM, labeled for 5 min with [^{35}S]methionine in the continued presence or absence of the compounds, and analyzed by immunoprecipitation, gel electrophoresis and autoradiography. p1 and pp indicate glycosylated proCPY in the ER lumen and untranslocated preproCPY. g and u indicate the glycosylated and unglycosylated forms of DPAPB. The position of molecular mass standards with their weight in kDa is indicated. (B) Dose-dependence of translocation inhibition for DPAPB and CPY was analyzed by metabolic labeling as above, using the indicated concentrations of compound 1 or 2 after preincubation for 30 min. 0 and 0* indicate labeling without or with DMSO, respectively, in the absence of inhibitors. (C) The time-course of inhibition was analyzed by metabolic labeling of DPAPB and CPY, as above, using a fixed concentration of 10 μM compound 1 or compound 2, and the indicated preincubation times of 0–30 min. (D) Quantification of translocation inhibition experiments as in C. Squares are used for DPAPB, circles for CPY, open symbols for compound 1, and filled symbols for compound 2. The mean±s.d. of two independent experiments are shown. (E) H1*, a protein derived from the mammalian type II membrane protein H1, with its natural signal-anchor sequence, or generic hydrophobic sequences composed of Leu_{13} or Leu_{16} were expressed in yeast and analyzed for inhibition of translocation by compounds 1 and 2 as in A. The unglycosylated, and the two- and three-fold glycosylated forms are indicated by 0, 2 and 3, respectively. (F) To analyze the effect on translocation in mammalian cells, COS-1 cells were transfected to express the asialoglycoprotein receptor H1 or derivatives in which the hydrophobic core of its signal-anchor was replaced by generic sequences of Leu_{13} or Leu_{25}. Cells were labeled for 30 min with [^{35}S]methionine in the presence or absence of the indicated concentrations of compound 1 or 2. H1 and its derivatives were immunoprecipitated and analyzed by gel electrophoresis and autoradiography. (G) To analyze inhibition of translocation in *E. coli*, purified SecA and SecYEG derivatives [full-length lacking cysteine residues (ΔCys and WT) or with deletion of plug residues 60–74 (Δ60-74 and ΔPlug)] were reconstituted into proteolipsomes. Radiolabeled proOmpA-DHFR (a post-translationally translocated fusion protein) was incubated in the presence of the indicated compound concentrations with ATP or without (–ATP). Translocation of the substrate was measured by proteinase K treatment followed by gel electrophoresis and autoradiography. The presented dose–response curves are mean±s.d. based on quantification of three experiments. (H) Sec61p mutants isolated by their resistance to 30 μM compound 1 were analyzed for their ability to suppress the translocation defect of CPYΔ3 (CPY with a mutant signal sequence lacking three apolar residues) by analyzing metabolic labeling of cells expressing CPYΔ3 or, as a control, CPY for 5 min, followed by immunoprecipitation, SDS-gel electrophoresis, and autoradiography. Glycosylation to the p1 forms indicates translocation into the ER lumen, whereas the unglycosylated preproCPY form is cytosolic. As a control, the material in the first lane was deglycosylated by endoglycosidase H (endoH) digestion. The fraction of translocated products is indicated as the percentage of the total (mean±s.d.; n=3).

translocation pore. The signal-anchor of TNFα could be crosslinked – preferentially by its C-terminal end and in a pattern suggesting a helical conformation – with cysteine residues engineered into Sec61α at the cytosolic top of the lateral gate (MacKinnon et al., 2014). To understand how the inhibitor blocks signal insertion we identified the resistance mutations. The five mutations causing resistance to cotransin CT08 recently published by MacKinnon et al. (MacKinnon et al., 2014) localize to the plug and to the lumenal end of the lateral gate helices TM2 and TM3. The conspicuous concentration to plug and lower gate suggested that this part of the structure constitutes the cotransin-binding site. Given that the affected residues point to the interior of the translocon in the closed state, the inhibitor could only bind there directly in an open conformation. Inhibitor binding was thus proposed to stabilize the plug and the partially opened gate, thereby preventing the signal from entering. The five mutations identified independently in human Sec61α1 in our study also localize to the same region, all in the plug domain. R66 was mutated in both studies to a total of three different residues (I, G and K). Given that the various affected plug residues point in very different directions, they are not likely to all contact the inhibitor directly.

In yeast, we identified a higher number of 22 mutations in 21 different residues conferring resistance to decatransin and/or cotransins; 16 mutations in 15 different residues were resistant to both chemotypes, indicating similar mechanisms of action. Several mutations also localize to the plug and gate region. In some instances, the same homologous residues were mutated, in one case even with the same amino acid exchange (S72F in yeast and S71F in human). However, the yeast mutations are distributed over a larger area than could be covered by a compact cyclic deca- or hepta-depsipeptide, suggesting conformational or allosteric effects to cause resistance by many mutations.

A variety of different mutations have previously been found to mediate the suppression of signal peptide defects, the *prl* ('protein localization') phenotype described in bacteria (Emr et al., 1981; Junne et al., 2007; Smith et al., 2005) and yeast (Junne et al., 2007). *prl* mutations specifically destabilize the closed state of the translocon, facilitating signal entry and initiation of peptide insertion and translocation. Mutations of the plug domain, constriction ring residues or of the lateral gate showed this phenotype, as well as mutations at other positions. The fact that almost all *prl* mutants showed some level of resistance to inhibition might be explained by 'flexibilization' of the interaction surfaces to reduce the binding affinity of the inhibitors. This might suggest that the inhibitors bind to the closed translocon or an early state of channel opening and stabilize it, thereby preventing signal insertion.

It is striking that both decatransin and cotransins inhibit translocons as distant in evolution as *E. coli*, yeast and man. Although the Sec61α subunit shares almost 60% identity between yeast and man (including 11 of 16 residues of the plug domain), there is less than 17% identity between the two eukaryotic sequences and bacterial SecY, with no sequence conservation in the plug. It thus appears unlikely that there are conserved specific inhibitor–protein interactions. Like signal sequences, the inhibitors are oligopeptides of hydrophobic (although in part unusual) amino acids. It is conceivable that they engage with the translocon in a similar manner as natural signals do – up to the point where their circular structure prevents the next step, such as the formation of an extended helix to intercalate into the lateral gate and contact the lipid phase. This state might block the translocon for an incoming signal. Destabilizing mutations (including the *prl* mutants) might allow for sufficient flexibility in the translocon to rapidly release the depsipeptides. According to this hypothesis, mutations that directly block inhibitor binding would also interfere with signal entry and might not be viable.

MATERIALS AND METHODS

Producer strain isolation and full genome sequencing

A fungal strain closely related to *Chaetosphaeria tulasneorum*, as determined by Internal Transcribed Spacer sequencing (White et al., 1990), was isolated from maple leaf debris in Germany. The genome was determined using Roche/454 sequencing and the Roche/454 Newbler assembler v.2.6. Two sequencing libraries were prepared, one shotgun library which generated 1,277,077 reads with an average read length of

Journal of Cell Science (2015) 128, 1217–1229 doi:10.1242/jcs.165746

Table 2. Inhibitor sensitivity of previously described Sec61 mutants

Sec61 mutation	Color code[a]	*prl*	CPY translation defect	Compound 1				Compound 2			
				IC_{50}* [μM]	r^2**	IC_{50} ratio to control	Phenotype	IC_{50}[b] [μM]	r^2[c]	IC_{50} ratio to control	Phenotype
Wild-type	–	–	–	0.8	0.995	1	S	0.7	0.998	1	S
6×A	Red	+	–	>100	–	>100	R	>100	–	>100	R
6×G	Red	+	(+)	>100	–	>100	R	>100	–	>100	R
6×S	Red	+	(+)	>100	–	>100	R	>100	–	>100	R
6×W	Red	±	(+)	>100	–	>100	R	>100	–	>100	R
Δplug	Red	+	(+)	>100	–	>100	R	>100	–	>100	R
Δtip	Red	+	+	>100	–	>100	R	>100	–	>100	R
ΔTM2	–	n.d.	+	>100	–	>100	R	>100	–	>100	R
W35R	–	–	–	0.8	0.994	1	S	0.5	0.975	0.71	S
D61N	Red	+	–	>100	–	>100	R	>100	–	>100	R
L63N	Red	+	–	2.9	0.978	3.63	(R)	>100	–	>100	R
R67C	Red	+	+	>100	–	>100	R	>100	–	>100	R
E79G	Red	+	–	>100	–	>100	R	>100	–	>100	R
I86T	–	+	–	1.5	0.991	1.88	S	0.4	0.989	0.57	S
I91T	–	–	+	1.1	0.972	1.38	S	0.2	0.804	0.29	HS
Q93R	–	–	–	1	0.986	1.25	S	0.4	0.974	0.57	S
Q96R	–	–	–	0.8	0.993	1	S	0.7	0.997	1	S
L131P	Orange	+	–	0.6	0.974	0.75	S	>100	–	>100	R
S161T	Orange	+	–	0.5	0.967	0.63	S	>100	–	>100	R
D168A	–	–	–	1	0.976	1.25	S	0.4	0.982	0.57	S
T185K	Blue	–	–	>100	–	>100	R	>100	–	>100	R
P200L	–	±	–	1.1	0.981	1.38	S	0.8	0.998	1.14	S
K284E	Green	±	–	1.1	0.971	1.38	S	1.6	0.977	2.29	(R)
P292S	–	–	+	1.3	0.981	1.63	S	0.8	0.979	1.14	S
M400K	–	–	–	0.8	0.991	1	S	0.7	0.999	1	S
M450K	Blue	–	–	3.2	0.893	4	(R)	2.2	0.968	3.14	(R)

These Sec61 mutants have previously been characterized by Junne et al. (Junne et al., 2006; Junne et al., 2007; Junne et al., 2010). *prl* phenotype and CPY translocation defects were analyzed by Junne et al. (Junne et al., 2007). S, sensitive; HS, hypersensitive (IC_{50} at least two-fold lower than wild-type); R, resistant; (R), moderately resistant (IC_{50} at least two-fold higher than wild-type); n.d., not determined. [a]The color code of mutations conferring resistance to at least one compound corresponds to that used in Fig. 3A, lower panel; [b]corresponding IC_{50} curves are shown in supplementary material Fig. S3; [c]r^2 values are shown where a sigmoidal curve could be fitted.

676 bp, and a paired-end library with pair distance average of 2768 bp and a pair distance standard deviation of 692 bp. The paired-end library was sequenced twice, yielding a total of 953,342 paired reads with a peak depth of 29. Sequences were assembled using the Newbler 2.6 assembler with default options, except for specifying the scaffolding and four processors. A total of 50 scaffolds were generated, with an average size of 843,301 bp and an N50 of 2,374,876 bp (the average contig size within these scaffolds was 124,629 bp; N50 scaffold contig size

Table 3. Identified SEC61A1 mutations in compound 2-resistant HCT116 colonies

Colony#	Mutation in Sec61α1	Codon change	Sequencing	Cluster	Compound 1		Compound 2	
					IC_{50}[a] (μM)	r^2[b]	IC_{50}[a] (μM)	r^2[b]
WT	–	–	–	–	0.14	0.99	0.05	0.97
1	S71F	TCT>TTT	Genome-wide	1	0.25	0.99	22.28	0.99
2	M65R	ATG>AGG	Genome-wide	5	0.79	>0.99	>30	–
3	R66I	AGA >ATA	Genome-wide	8	0.18	0.99	7.63	0.99
4	M65R	ATG>AGG	Genome-wide	5	0.81	>0.99	>30	–
5	D60E	GAC>GAA	Genome-wide	3	0.42	0.99	7.31	0.99
6	D60E	GAC>GAA	Genome-wide	3	0.48	0.99	8.71	0.99
7	D60G	GAC>GGC	Genome-wide	6	6.22	>0.99	>30	–
8	S71F	TCT>TTT	Genome-wide	2	0.37	0.98	8.56	0.99
9	None		Genome-wide	4	0.6	0.99	12.15	0.98
10	None		Genome-wide	7	1.04	>0.99	12.12	0.98
11	S71P	TCT>CCT	SEC61A1	–	0.55	>0.99	>30	–
12	S71P	TCT>CCT	SEC61A1	–	–	–	–	–
13	S71F	TCT>TTT	SEC61A1	–	–	–	–	–
14	S71F	TCT>TTT	SEC61A1	–	–	–	–	–
15	I41D; R66K	ATC>AAC; AGA>AAA	SEC61A1	–	0.11	0.99	10.61	0.99
16	I41D; R66K	ATC>AAC; AGA>AAA	SEC61A1	–	–	–	–	–

For description of colony genotype analysis, see Materials and Methods. [a]Corresponding IC_{50} curves are shown in Fig. 4A,B; [b]r^2 values are shown where a sigmoid curve could be fitted.

594,413 bp). Gene modeling and prediction of the genome was undertaken using Augustus (Keller et al., 2011). Augustus must be trained on each new fungus, and we used the CEGMA software (Parra et al., 2007) to provide an initial training set of spliced genes. In parallel, total RNA was isolated from the fungus using the RNeasy plant mini kit (Qiagen). RNA-seq libraries were prepared using an Illumina RNA prep kit, and sequenced using the Illumina HiSeq2000 platform. A total of 80 million 76-bp paired-end reads were generated. We supplemented the genome data with RNAseq following the Augustus RNAseq tutorial.

Using the gene predictions from Augustus, we predicted protein sequences. In addition, we identified all open reading frames >500 amino acids within the genome. Finally, we used Tophat 2.0.4 (http://ccb.jhu.edu/software/tophat/index.shtml) and Cufflinks 2.0.2 (http://cufflinks.cbcb.umd.edu) to identify the putative transcripts in the mRNA sample, and protein sequences were predicted from these. Using NCBI Blast with both Swissprot and the NCBI Non-Redundant protein data files, the predicted sequences were annotated. AntiSMASH was used to find secondary metabolite gene clusters.

Fermentation conditions, compound purification and structure elucidation

The strain was cultivated in 200-ml shake flasks with 60 ml main culture medium (yeast extract 2 g/l, malt extract 1.6 g/l, soy protein 2 g/l, glucose 20 g/l, $MgSO_4$ 2 g/l, KH_2PO_4 2 g/l) at 28℃ and 200 rpm for 8 days after inoculation with 1.5 ml of a 6-day preculture (agar 1 g/l, yeast extract 4 g/l, malt extract 15.6 g/l). Compounds were isolated by normal and reversed phase chromatography. The structure was determined by mass spectroscopy and 1D- and 2D-NMR experiments. The spectroscopic methods structural and spectral data for compound 1 can be found in the supplementary materials (supplementary material Table S2).

Chemogenomic profiling – HIP and HOP

The growth-inhibitory potency of test substances was determined using wild-type *S. cerevisiae* BY4743. The optical density at 600 nm (OD_{600}) of exponentially growing cultures in rich medium was recorded with a robotic system. Twelve-point serial dilutions were assayed in 96-well plates with a reaction volume of 150 µl; the start OD_{600} was 0.05. Solutions containing DMSO were normalized to 2%. IC_{30} values were calculated using logistic regression curve fits generated by TIBCO Spotfire v3.2.1 (TIBCO Software Inc.).

HIP, HOP and microarray analysis were performed as described previously (Hoepfner et al., 2014). Sensitivity was computed as the median absolute deviation logarithmic (MADL) score for each compound and concentration combination. *z*-scores are based on a robust parametric estimation of gene variability from >3000 different profilings and were computed as described in detail in previously (Hoepfner et al., 2014).

Growth curves

HIP and HOP profiles were validated by picking the individual strains from the HIP and HOP collections (OpenBiosystems, cat. number YSC1056 and YSC1055) and testing log-phase cultures in 96-well microtiter plates in YPD medium with serial dilutions of the compound. The assay volume was 150 µl/well, start OD_{600} was 0.01, DMSO was normalized to 2%. Curves were calculated by taking the 11 h OD_{600} measurements and applying a logistic regression curve fit in TIBCO Spotfire v3.2.1. Strain *HO/YDL228C* was used as the wild-type reference.

Selection of resistant *S. cerevisiae* cells

Strain BY4743Δ8 (Hoepfner et al., 2012) was incubated with 2.5% EMS until only 50% of the cells formed colonies. A total of 2×10^7 mutagenized cells were plated on two 14-cm dishes with synthetic complete medium (0.7 g/l Difco Yeast Nitrogen Base without amino acids, 0.79 g/l MPbio CSM amino acid mixture, 2% glucose) containing 30 µM compound 1. After 4 days, 45 resistant colonies were isolated. Resistance due to mutated *SEC61* was confirmed by cloning the corresponding mutations into fresh BY4743 cells and recording dose–response curves in YPD medium with serial dilutions of compounds 1 or 2 at 200 µM maximum concentration and 11 serial dilutions. DMSO was normalized to 2%. Curves were fitted by logistic regression curve fitting in TIBCO Spotfire v3.2.1 (TIBCO Software Inc.).

Selection and sequencing of resistant HCT116 cells

HCT116 cells were mutagenized by incubating with 2% EMS for 60 min aiming to kill 30% of the cells. A total of 1×10^7 mutagenized cells were plated and allowed to recover for 1.5 doubling times under standard conditions (10% FBS supplemented medium, 5% CO_2, 37℃). Compound 2 was added at the minimal inhibitory concentration (MIC; 1 µM) when they were 50–80% confluent, and medium was changed every 3–4 days. Resistant colonies appeared within 2–4 weeks. Resistance was confirmed by retesting the cells for growth in a dilution series from one tenth to one hundred times the IC_{50} (0.3 µM). For growth assays, CellTiter-Glo (Promega) cell viability assay reagent was used according to the manufacturer's instructions. The envision system was used for the readout, and IC_{50} values were determined by using the logistic regression curve fit function in TIBCO Spotfire v3.2.1.

Stable resistant colonies were tested in growth curves with compound 1, compound 2 and taxol. Ten colonies were expanded to extract genomic DNA and total RNA for sequencing using the Qiagen ALL Prep DNA/RNA kit (Qiagen) and were quantified by Qubit Fluorometric quantification (Life Technologies). 100 ng DNA was fragmented using a Covaris E210 ultrasonicator to an average length of 300 bp. The DNA was end-repaired, and Illumina-compatible sequencing libraries were prepared using the NuGen DR ultralow library kit. Libraries were then multiplexed and captured using a combination of NuGen blockers and Agilent SureSelect XT capture oligonucleotides following the NuGen recommendations. Libraries for transcriptome sequencing were prepared using the TruSeq v2 mRNA sequencing protocol (Ilumina Corp.). Sequencing was performed on an Illumina HiSeq2500 using TruSeq v3 sequencing chemistry on a HiSeq v3 paired end flowcell. The read length for all sequencing runs was 2× 76 bp, according to manufacturer's instructions (Illumina). Sample demultiplexing was performed using CASAVA v1.8.2 with FASTQC v0.10.0.

SNP analysis

The raw sequence reads were aligned to the human genome (hg19) using BWA version 0.5.9 (Li and Durbin, 2009). SNPs were called in two different ways. GATK version 1.6-11 was used to call SNPs for each of the resistant samples as well as for two samples of the unmutagenized reference strain HCT116 (McKenna et al., 2010). The SNPs of the two reference strain samples were then subtracted from the SNPs of the resistant samples. Secondly, we used a slightly modified version of the SNP calling method described previously (Wacker et al., 2012) to obtain SNPs at positions where the resistant mutant differs from the parental strain. SNPs were only kept if called against both of the reference strain samples. The combined set of SNPs from both methods was annotated using VEP for Ensembl v71 (Li and Durbin, 2009; McKenna et al., 2010; McLaren et al., 2010).

In vivo translocation assays in yeast and COS-1 cells

Yeast strain RSY1293 {matα, *ura3-1*, *leu2-3,-112*, *his3-11,-15*, *trp1-1*, *ade2-1*, *can1-100*, *sec61::HIS3*, [YCplac111 (*LEU2 CEN*) containing *SEC61*]} was used (Pilon et al., 1997). The substrate proteins dipeptidyl aminopeptidase B (DPAPB), carboxypeptidase Y (CPY), and CPYΔ3 with C-terminal triple HA epitope tags were described by Junne et al. (Junne et al., 2007), and H1* and derivatives by Goder et al. (Goder et al., 2004). All were cloned into pRS426 with a GPD promoter. Yeast cells expressing substrate proteins were *in vivo* pulse-labeled for 5 min with 150 µCi/ml [^{35}S]methionine and [^{35}S]cysteine (PerkinElmer Life and Analytical Sciences, Boston, MA), lysed with glass beads, heated to 95℃ for 5 min with 1% SDS, cleared by centrifugation, subjected to immunoprecipitation, and analyzed by SDS-gel electrophoresis and autoradiography as described previously (Junne et al., 2006). Compound 1 and 2 were added in DMSO (≤1% of the medium) 0–30 min before and during the labeling period. Signals were quantified using a phosphoimager. Mutant *sec61* sequences were cloned into YCplac111 (*LEU2 CEN*) and introduced into VGY61 {matα, *ura3-1*, *leu2-3,-112*,

his3-11,-15, *trp1-1*, *ade2-1*, *can1-100*, *sec61::HIS3*, [YCPlac33 (*URA3 CEN*) containing *SEC61*]} (Goder et al., 2004), and the wild-type *SEC61* plasmid was eliminated using 5-fluororotic acid for metabolic labeling experiments. COS-1 cells were grown, transfected, and labeled as previously described (Goder and Spiess, 2003). Inhibitors were added in DMSO (≤1% of the medium) during the labeling period. H1, H1Leu13, and H1Leu25 were as described previously (Wahlberg and Spiess, 1997).

Bacterial *in vitro* translocation assay

In vitro translocation assays with purified components from *Escherichia coli* were performed essentially as described previously (Bauer et al., 2014). SecA (residues 1–831 with all cysteine residues replaced by serine residues and a C-terminal His_6 tag) and SecYEG (with all cysteine residues replaced by serine residues and with a N-terminal His_6 tag in SecE) as well as a derivative in which the plug domain of SecY (residues 60–74) was deleted were purified. The SecYEG complexes were reconstituted into proteolipsomes containing *E. coli* polar lipid extract. pOA-DHFR, a fusion of the first 175 amino acids of proOmpA and *E. coli* dihydrofolate reductase, was synthesized and radiolabeled with [^{35}S]methionine by *in vitro* translation with rabbit reticulocyte lysate (Promega) as described previously (Bauer and Rapoport, 2009).

Proteoliposomes containing 0.1 µM SecYEG were mixed with 0.4 µM SecA, 5 mM ATP and pOA-DHFR diluted 1:50 from the reticulocyte lysate in buffer containing 50 mM Hepes-NaOH pH 7.5, 50 mM KCl and 5 mM $MgCl_2$. The mixture was split into equal volumes and incubated with different concentrations of compounds 1 or 2 or DMSO for 30 s on ice. Translocation was then initiated by incubation for 5 min at 37℃. Translocation of pOA-DHFR was tested by proteinase K treatment followed by SDS-PAGE and autoradiography.

Acknowledgements

We would like to acknowledge the Novartis Extended Natural Products Unit team that supported fermentation, isolation, and characterization of the compounds used in this study.

Competing interests

J.W., C.S., T.A., M.B., B. Bhullar, J.E., D.E., N.H., B.K., P.K., N.M., E.O., L.O., R.R., G.R., S.S., F.P., J.T. and D.H. are employees of Novartis. R.B. is an employee of Congenomics. The other authors declare no competing or financial interests.

Author contributions

T.A., B. Bauer, J.E., D.E., B.K., P.K., N.M., E.O., R.R., and C.S. performed experiments. B. Bhullar, N.H., F.P., T.A.R. and J.T. designed experiments. M.B., R.B., L.O., G.R., S.S. analyzed experiments. T.J. and J.W. performed and analyzed experiments. D.H. and M.S. designed and analyzed experiments, and wrote the manuscript.

Funding

This work was supported by the Swiss National Science Foundation [grant number 31003A-125423 to M.S.]; and a grant from the National Institutes of Health [grant number GM052586] to T.A.R. T.A.R. is a Howard Hughes Medical Institute Investigator. B. Bauer was supported by a Ph.D. fellowship of the Boehringer Ingelheim Fonds. Deposited in PMC for release after 6 months.

Supplementary material

Supplementary material available online at
http://jcs.biologists.org/lookup/suppl/doi:10.1242/jcs.165746/-/DC1

Reference

Bachmann, B. O. and Ravel, J. (2009). Chapter 8. Methods for in silico prediction of microbial polyketide and nonribosomal peptide biosynthetic pathways from DNA sequence data. *Methods Enzymol.* **458**, 181-217.

Bauer, B. W. and Rapoport, T. A. (2009). Mapping polypeptide interactions of the SecA ATPase during translocation. *Proc. Natl. Acad. Sci. USA* **106**, 20800-20805.

Bauer, B. W., Shemesh, T., Chen, Y. and Rapoport, T. A. (2014). A ''push and slide'' mechanism allows sequence-insensitive translocation of secretory proteins by the SecA ATPase. *Cell* **157**, 1416-1429.

Bender, A. and Glen, R. C. (2004). Molecular similarity: a key technique in molecular informatics. *Org. Biomol. Chem.* **2**, 3204-3218.

Besemer, J., Harant, H., Wang, S., Oberhauser, B., Marquardt, K., Foster, C. A., Schreiner, E. P., de Vries, J. E., Dascher-Nadel, C. and Lindley, I. J. (2005). Selective inhibition of cotranslational translocation of vascular cell adhesion molecule 1. *Nature* **436**, 290-293.

Cross, B. C., McKibbin, C., Callan, A. C., Roboti, P., Piacenti, M., Rabu, C., Wilson, C. M., Whitehead, R., Flitsch, S. L., Pool, M. R. et al. (2009). Eeyarestatin I inhibits Sec61-mediated protein translocation at the endoplasmic reticulum. *J. Cell Sci.* **122**, 4393-4400.

Emr, S. D., Hanley-Way, S. and Silhavy, T. J. (1981). Suppressor mutations that restore export of a protein with a defective signal sequence. *Cell* **23**, 79-88.

Field, B., Cardon, G., Traka, M., Botterman, J., Vancanneyt, G. and Mithen, R. (2004). Glucosinolate and amino acid biosynthesis in Arabidopsis. *Plant Physiol.* **135**, 828-839.

Gao, X., Haynes, S. W., Ames, B. D., Wang, P., Vien, L. P., Walsh, C. T. and Tang, Y. (2012). Cyclization of fungal nonribosomal peptides by a terminal condensation-like domain. *Nat. Chem. Biol.* **8**, 823-830.

Garrison, J. L., Kunkel, E. J., Hegde, R. S. and Taunton, J. (2005). A substrate-specific inhibitor of protein translocation into the endoplasmic reticulum. *Nature* **436**, 285-289.

Giaever, G., Shoemaker, D. D., Jones, T. W., Liang, H., Winzeler, E. A., Astromoff, A. and Davis, R. W. (1999). Genomic profiling of drug sensitivities via induced haploinsufficiency. *Nat. Genet.* **21**, 278-283.

Goder, V. and Spiess, M. (2003). Molecular mechanism of signal sequence orientation in the endoplasmic reticulum. *EMBO J.* **22**, 3645-3653.

Goder, V., Junne, T. and Spiess, M. (2004). Sec61p contributes to signal sequence orientation according to the positive-inside rule. *Mol. Biol. Cell* **15**, 1470-1478.

Gogala, M., Becker, T., Beatrix, B., Armache, J. P., Barrio-Garcia, C., Berninghausen, O. and Beckmann, R. (2014). Structures of the Sec61 complex engaged in nascent peptide translocation or membrane insertion. *Nature* **506**, 107-110.

Harant, H., Lettner, N., Hofer, L., Oberhauser, B., de Vries, J. E. and Lindley, I. J. (2006). The translocation inhibitor CAM741 interferes with vascular cell adhesion molecule 1 signal peptide insertion at the translocon. *J. Biol. Chem.* **281**, 30492-30502.

He, M. (2006). Pipecolic acid in microbes: biosynthetic routes and enzymes. *J. Ind. Microbiol. Biotechnol.* **33**, 401-407.

Hoepfner, D., McNamara, C. W., Lim, C. S., Studer, C., Riedl, R., Aust, T., McCormack, S. L., Plouffe, D. M., Meister, S., Schuierer, S. et al. (2012). Selective and specific inhibition of the plasmodium falciparum lysyl-tRNA synthetase by the fungal secondary metabolite cladosporin. *Cell Host Microbe* **11**, 654-663.

Hoepfner, D., Helliwell, S. B., Sadlish, H., Schuierer, S., Filipuzzi, I., Brachat, S., Bhullar, B., Plikat, U., Abraham, Y., Altorfer, M. et al. (2014). High-resolution chemical dissection of a model eukaryote reveals targets, pathways and gene functions. *Microbiol. Res.* **169**, 107-120.

Hoon, S., Smith, A. M., Wallace, I. M., Suresh, S., Miranda, M., Fung, E., Proctor, M., Shokat, K. M., Zhang, C., Davis, R. W. et al. (2008). An integrated platform of genomic assays reveals small-molecule bioactivities. *Nat. Chem. Biol.* **4**, 498-506.

Junne, T., Kocik, L. and Spiess, M. (2010). The hydrophobic core of the Sec61 translocon defines the hydrophobicity threshold for membrane integration. *Mol. Biol. Cell* **21**, 1662-1670.

Junne, T., Schwede, T., Goder, V. and Spiess, M. (2006). The plug domain of yeast Sec61p is important for efficient protein translocation, but is not essential for cell viability. *Mol. Biol. Cell* **17**, 4063-4068.

Junne, T., Schwede, T., Goder, V. and Spiess, M. (2007). Mutations in the Sec61p channel affecting signal sequence recognition and membrane protein topology. *J. Biol. Chem.* **282**, 33201-33209.

Keller, O., Kollmar, M., Stanke, M. and Waack, S. (2011). A novel hybrid gene prediction method employing protein multiple sequence alignments. *Bioinformatics* **27**, 757-763.

Li, H. and Durbin, R. (2009). Fast and accurate short read alignment with Burrows-Wheeler transform. *Bioinformatics* **25**, 1754-1760.

Liu, Y., Law, B. K. and Luesch, H. (2009). Apratoxin a reversibly inhibits the secretory pathway by preventing cotranslational translocation. *Mol. Pharmacol.* **76**, 91-104.

MacKinnon, A. L., Garrison, J. L., Hegde, R. S. and Taunton, J. (2007). Photo-leucine incorporation reveals the target of a cyclodepsipeptide inhibitor of cotranslational translocation. *J. Am. Chem. Soc.* **129**, 14560-14561.

MacKinnon, A. L., Paavilainen, V. O., Sharma, A., Hegde, R. S. and Taunton, J. (2014). An allosteric Sec61 inhibitor traps nascent transmembrane helices at the lateral gate. *eLife* **3**, e01483.

Maifeld, S. V., MacKinnon, A. L., Garrison, J. L., Sharma, A., Kunkel, E. J., Hegde, R. S. and Taunton, J. (2011). Secretory protein profiling reveals TNF-α inactivation by selective and promiscuous Sec61 modulators. *Chem. Biol.* **18**, 1082-1088.

McKenna, A., Hanna, M., Banks, E., Sivachenko, A., Cibulskis, K., Kernytsky, A., Garimella, K., Altshuler, D., Gabriel, S., Daly, M. et al. (2010). The Genome Analysis Toolkit: a MapReduce framework for analyzing next-generation DNA sequencing data. *Genome Res.* **20**, 1297-1303.

McLaren, W., Pritchard, B., Rios, D., Chen, Y., Flicek, P. and Cunningham, F. (2010). Deriving the consequences of genomic variants with the Ensembl API and SNP Effect Predictor. *Bioinformatics* **26**, 2069-2070.

Nyfeler, B., Hoepfner, D., Palestrant, D., Kirby, C. A., Whitehead, L., Yu, R., Deng, G., Caughlan, R. E., Woods, A. L., Jones, A. K. et al. (2012). Identification of elongation factor G as the conserved cellular target of argyrin B. *PLoS ONE* **7**, e42657.

Park, E. and Rapoport, T. A. (2011). Preserving the membrane barrier for small molecules during bacterial protein translocation. *Nature* **473**, 239-242.
Park, E. and Rapoport, T. A. (2012). Mechanisms of Sec61/SecY-mediated protein translocation across membranes. *Annu. Rev. Biophys.* **41**, 21-40.
Park, E., Ménétret, J. F., Gumbart, J. C., Ludtke, S. J., Li, W., Whynot, A., Rapoport, T. A. and Akey, C. W. (2014). Structure of the SecY channel during initiation of protein translocation. *Nature* **506**, 102-106.
Parra, G., Bradnam, K. and Korf, I. (2007). CEGMA: a pipeline to accurately annotate core genes in eukaryotic genomes. *Bioinformatics* **23**, 1061-1067.
Pilon, M., Schekman, R. and Römisch, K. (1997). Sec61p mediates export of a misfolded secretory protein from the endoplasmic reticulum to the cytosol for degradation. *EMBO J.* **16**, 4540-4548.
Richie, D. L., Thompson, K. V., Studer, C., Prindle, V. C., Aust, T., Riedl, R., Estoppey, D., Tao, J., Sexton, J. A., Zabawa, T. et al. (2013). Identification and evaluation of novel acetolactate synthase inhibitors as antifungal agents. *Antimicrob. Agents Chemother.* **57**, 2272-2280.
Sadlish, H., Galicia-Vazquez, G., Paris, C. G., Aust, T., Bhullar, B., Chang, L., Helliwell, S. B., Hoepfner, D., Knapp, B., Riedl, R. et al. (2013). Evidence for a functionally relevant rocaglamide binding site on the eIF4A-RNA complex. *ACS Chem. Biol.* **8**, 1519-1527.
Shao, S. and Hegde, R. S. (2011). Membrane protein insertion at the endoplasmic reticulum. *Annu. Rev. Cell Dev. Biol.* **27**, 25-56.
Shimada, K., Filipuzzi, I., Stahl, M., Helliwell, S. B., Studer, C., Hoepfner, D., Seeber, A., Loewith, R., Movva, N. R. and Gasser, S. M. (2013). TORC2 signaling pathway guarantees genome stability in the face of DNA strand breaks. *Mol. Cell* **51**, 829-839.
Smith, M. A., Clemons, W. M., Jr, DeMars, C. J. and Flower, A. M. (2005). Modeling the effects of prl mutations on the Escherichia coli SecY complex. *J. Bacteriol.* **187**, 6454-6465.
Stachelhaus, T., Mootz, H. D. and Marahiel, M. A. (1999). The specificity-conferring code of adenylation domains in nonribosomal peptide synthetases. *Chem. Biol.* **6**, 493-505.
Voorhees, R. M., Fernández, I. S., Scheres, S. H. and Hegde, R. S. (2014). Structure of the mammalian ribosome-Sec61 complex to 3.4 Å resolution. *Cell* **157**, 1632-1643.
Wacker, S. A., Houghtaling, B. R., Elemento, O. and Kapoor, T. M. (2012). Using transcriptome sequencing to identify mechanisms of drug action and resistance. *Nat. Chem. Biol.* **8**, 235-237.
Wahlberg, J. M. and Spiess, M. (1997). Multiple determinants direct the orientation of signal-anchor proteins: the topogenic role of the hydrophobic signal domain. *J. Cell Biol.* **137**, 555-562.
Westendorf, C., Schmidt, A., Coin, I., Furkert, J., Ridelis, I., Zampatis, D., Rutz, C., Wiesner, B., Rosenthal, W., Beyermann, M. et al. (2011). Inhibition of biosynthesis of human endothelin B receptor by the cyclodepsipeptide cotransin. *J. Biol. Chem.* **286**, 35588-35600.
White, T. J., Bruns, T., Lee, S. and Taylor, J. (1990). Amplification and direct sequencing of fungal ribosomal RNA genes for phylogenetics. In *PCR Protocols: A Guide to Methods and Applications* (ed. M. A. Innis, D. H. Gelfand, J. J. Sninsky and T. J. White), pp. 315-322. San Diego, CA: Academic press Inc.